

CAM-LEM PROCESSING: MATERIALS FLEXIBILITY

Z. E. Liu, T. C. Ko, J. Best, J. D. Cawley, and A. H. Heuer
Department of Materials Science and Engineering
Case Western Reserve University
10900 Euclid Avenue
Cleveland OH 44106-7204

ABSTRACT

The cut-then-stack paradigm of computer-aided manufacturing of laminated engineering materials (CAM-LEM) offers choice of feedstock material, ease of handling finely divided (and therefore sinterable) powders, and the ability to mix materials. This combination of features was exploited to process fluidic devices. CAM-LEM processing was used to render the part in aluminum oxide, silicon nitride, and stainless steel.

INTRODUCTION

Computer-aided manufacturing of laminated engineering materials (CAM-LEM) has been developed as a solid freeform process to allow direct layered-manufacturing of components of complex geometry in any one of an array of engineering materials. To date, efforts has focussed on the use of powder-based processing of ceramics and metals.

When working in ceramics or metals using the CAM-LEM process, the method of part construction is robotic assembly of cut outlines followed by green-state lamination and conventional firing [1-4]. The feedstock for the process is a "green tape" that serves as a powder carrier. Separate preprocessing of the tape by methods such as tape casting [5] or compression molding [6] allows the process to employ finely divided powders (submicron, in the case of ceramics), creates uniform particle packing, and completely avoids problems associated with flow instabilities or segregation effects.

Powder-based tapes are widely used in industrial applications and a number of techniques have been developed for their production. Specific process selection is dependent on property requirements. For CAM-LEM processing, important tape characteristics include behavior during laser cutting and ease of lamination. It has been determined that some commercially available tape formulations are suitable for CAM-LEM processing, whereas others are not. In addition, tapes can be produced from either commercially compounded feedstocks or mixtures of raw materials.

Through the use of the cut-then-stack paradigm, CAM-LEM processing offers increased geometric flexibility relative to other forms of laminated object manufacturing. The ability to carry out "tangent cutting" yields improved surface finish and faithfulness in approximation of a CAD model [7-9]. Furthermore, the ready inclusion of a fugitive material during building allows parts to be built with highly complex interior surfaces [3,4].

DEFINITION OF TEST PART

One class of parts that are well suited to CAM-LEM processing are fluidics. These devices are used for a variety of purposes, but share a common operational characteristic; all operate by motion of a condensed fluid through a series of internal passages within the device under a pressure gradient. CAM-LEM processing is an appealing method for fabricating these parts because it allows integral fabrication (i.e., formation of a single monolithic piece with appropriate internal passages), thus mitigating the need separate processing of subcomponents and assembly, and increasing reliability. CAM-LEM also offers increased flexibility in material choice. The

material choice. The particular fluidic circuit selected for this study requires five layers, has a circular motif, and is disc-shaped with three fold rotational symmetry.

MATERIALS: SELECTION, PREPROCESSING, AND LAMINATION

Three materials were selected for construction: aluminum oxide, silicon nitride, and stainless steel. Silicon nitride powder (GS-44, AlliedSignal Ceramic Components, Torrance CA) was tape cast using a binder system based on polyvinyl butyral. Commercial (Coors Electronic Ceramics, Chattanooga) aluminum oxide tapes were used. These tapes were 96% alumina and fabricated by tape casting using a binder system also based on polyvinyl butyral. Stainless steel tapes were fabricated by compression molding using a developmental injection molding feedstock (Rohm and Haas, Springhouse PA). The steel powder was gas-atomized 316L and binder system in this case was determined to be based on polymethyl methacrylate. For working with both the silicon nitride and aluminum oxide tapes, a fugitive tape system based on graphite powder has been developed in-house. Characteristics for all tapes are given in Table 1.

Table 1. Green Tape Characteristics

<u>Tape</u>	<u>Thickness</u>	<u>Solids Loading</u>	<u>Binder Content</u>	<u>Porosity</u>
Aluminum Oxide	600 μm	56.6 vol. %	20.5 vol. %	22.9 %
Silicon Nitride	300	51.6	29.9	18.5
Stainless Steel	600	64.0	36.0	none
Graphite*	300 or 600	42.8	21.9	35.3

*Thicknesses were processed to match various feedstocks. For this system, all calculations assume a graphite density of 2.3 g/cc.

For all systems, lamination was achieved using a variant of the adhesive lamination process that has been reported elsewhere [10]. The specifics of the adhesive formulation were varied for each system in order to optimize lamination efficiency and to obtain process tolerance (e.g., allow good adhesion throughout a broader window in time after the adhesive formulation was applied). Both the nature of the organic “package” and the characteristics of the porosity influence the choice of adhesive.

CAM-LEM PROCESSED PARTS

Successful parts were produced from all three materials. Figure 1 shows the cut outlines for both the aluminum oxide and graphite fugitive. Figure 2a shows an assembled part made from aluminum oxide tape with a graphite fugitive. The fugitive plays two roles; it defines the internal passages and it serves as a pressure-transmitting medium during lamination. Figure 2b is an image of the same part after pyrolysis of the binder and removal of the fugitive have been effected. Note that the fugitive is always removed prior to the onset of macroscopic shrinkage. This is done to avoid the occurrence of backstresses or encapsulation of fugitive by a densifying matrix. Figure 2c is an image of the fully densified part, in which the nominally 17% linear shrinkage is observed.

Figure 3a and 3b are back lit images of the translucent aluminum oxide part from two sides, respectively. The interior passages are clearly imaged and these figures demonstrate that the details of the interior surface are well preserved during postprocessing, i.e., firing.

Similarly good results were obtained using silicon nitride. Figure 4 shows an image of one face of a completely processed part. The tearshaped contrast is produced by low-level carbon doping of the silicon nitride in the outer layer where it was in contact with the fugitive underneath. This has been shown not to affect the properties of the material [11]. As silicon nitride is opaque,

it was not possible to image the interior directly, but functionality was demonstrated by simple flow tests.

The stainless steel version of this part is shown in Figure 5a and 5b. A high quality part also was produced in this material.

High lamination efficiency was confirmed by sectioning and preparing the cut surfaces using standard metallographic techniques. External dimensions of aluminum oxide and silicon nitride were determined using a coordinate measuring machine. Line scans across the diameter of the face containing the larger orifice were collected from several aluminum oxide samples as well as one stainless steel, and a pseudo-2D map was generated of the same surface of a silicon nitride part. This surface was chosen, rather than the opposite, because the three teardrop-shaped voids in the second layer present a more critical test of the ability to process parts with interior channels.

The line scans from the alumina indicate that the inclusion of the fugitive does not significantly affect the tendency of the sample to slump during firing. Line scans revealed that a small amount of slumping, on the order of $150\ \mu\text{m}$ over a 15 mm span, occurred over internal cavities in all cases. A typical result is shown in Fig. 6. Similarly, the surface relief map of the silicon nitride part shows modest relief, see Fig. 7. The line scans from stainless steel part also show evidence of relief, but it is considerably more modest. The difference is attributed to the fact that both of the ceramics form an appreciable amount of liquid during firing (due to the presence of silicate sintering aids) whereas under the conditions used to sinter the stainless steel, the system remains completely solid. The results are entirely consistent with the expectations associated with these materials; the deformation during firing is comparable to that observed in these materials when conventionally processed.

CONCLUSIONS

The use of CAM-LEM processing to directly produce a component in a variety of structural materials has been demonstrated. Thus, CAM-LEM processing is an attractive method for conducting small scale production in the context of materials substitution trials.

A fugitive has been developed that is compatible with both aluminum oxide and silicon nitride. The fugitive has been used to produce integral parts with highly complex internal geometrical features.

ACKNOWLEDGEMENTS

This research was supported by the CAMP, Inc. Applied Research Program and the Office of Naval Research (ONR Grant Number N00014-95-10107). Aluminum oxide tape was supplied by Dr. Debra Horn of Coors Electronic Ceramics. Dr. John Pollinger, AlliedSignal Ceramic Components, supplied the silicon nitride powder and fired the silicon nitride parts. The stainless steel feedstock was supplied by Dr. Len Bogan of Rohm and Haas. Firing of the stainless steel parts was carried out at BFGoodrich, Brecksville OH, by Tom Nixon. Dr. Ajit Sane granted access to compression molding facilities at BP America. Finally, CAM-LEM is a multidisciplinary activity at Case Western Reserve University, we gratefully recognize the contributions of our colleagues in the Electrical Engineering and Applied Physics Department; Prof. W. S. Newman, Dr. Y. Zheng, and S. Choi.

REFERENCES

1. J. D. Cawley, Z. Liu, W. S. Newman, B. B. Mathewson, and A. H. Heuer, "Alumina Ceramics Made by CAM-LEM (Computer-Aided Manufacturing of Laminated Engineering Materials) Technology," Proc. Solid Freeform Fabrication Symp., Univ. Texas Austin, pgs. 9-16, (1995).

2. B. B. Mathewson, W. S. Newman, A. H. Heuer, and J. D. Cawley, "Automated Fabrication of Ceramic Components from Tape-Cast Ceramic," Proc. Solid Freeform Fabrication Symp., Univ. Texas Austin, pgs. 253-260 (1995).
3. Z. Z. Liu, P. Wei, B. Kernan, A. H. Heuer, and J. D. Cawley, "Metal and Ceramic Components Made via CAM-LEM Technology," Proc. Solid Freeform Fabrication Symp., Univ. Texas Austin, pg. 377-384 (1996).
4. J. D. Cawley, A. H. Heuer, W. S. Newman, and B. B. Mathewson, "Computer-Aided Manufacturing of Laminated Engineering Materials," Am. Ceram. Soc. Bull., 75 [5] 75-79 (1996).
5. J. S. Reed, Principles of Ceramic Processing, pgs. 525-534, John Wiley and Sons, New York (1995).
6. H. F. Mark et al., Encyclopedia of Polymer Science and Engineering Vol. 4, John Wiley and Sons, New York, pgs. 79-108, 1985.
7. Y. Zheng, S. Choi, B. Mathewson, and W. Newman, "Progress in Computer-Aided Manufacturing of Laminated Engineering Materials Utilizing Thick, Tangent-Cut Layers," Proc. Solid Freeform Fabrication Symp., University of Texas at Austin, perform Fabrication Symp., University of Texas at Austin, pg. 9-16 (1995).
8. Y. Zheng, PhD Dissertation, Case Western Reserve University, 1997.
9. Y. Zheng and W. S. Newman, "Software Design Challenges for Computer-Aided Manufacturing of Laminated Engineering Materials, Proc. 6th Eur. Conf. on Rapid Prototyping and Manuf., Univ. Nottingham, UK, pgs. 21-30, (1997).
10. P. Wei, J. D. Cawley, and A. H. Heuer, "CAM-LEM Processing: Lamination Technology," Proc. 6th Eur. Conf. on Rapid Prototyping and Manuf., Univ. Nottingham, UK, pgs. 95-104 (1997).
11. Personal communication, J. Pollinger, AlliedSignal Ceramic Components.

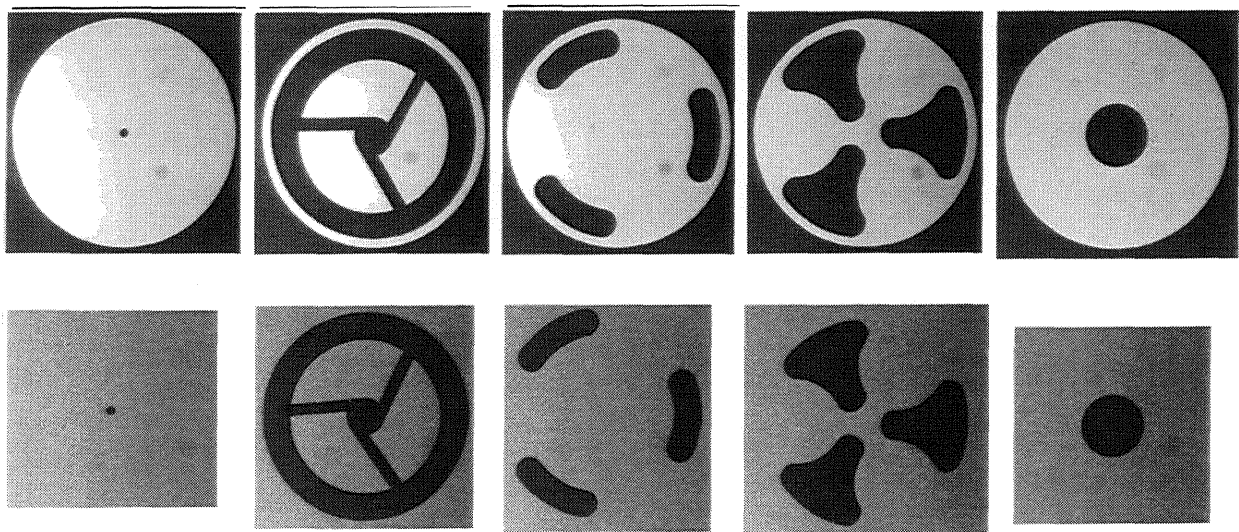


Figure 1 Digital photographs of the cut outlines forming the positive space (from alumina, upper series) and the negative space (from fugitive, lower series) of the fluidic circuit selected for study.

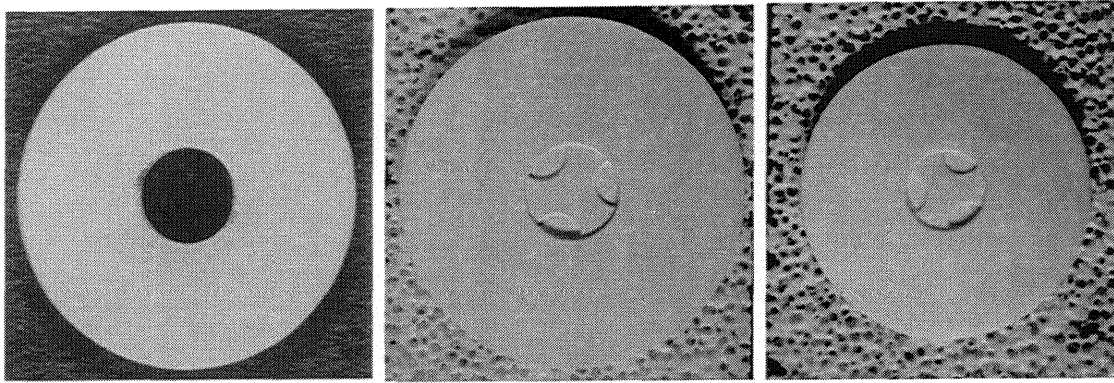


Figure 2 Aluminum oxide fluidic circuit after assembly. From left to right the images are: assembled with fugitive occupying the negative space, after heat treatment to remove binder and fugitive, and after complete densification.

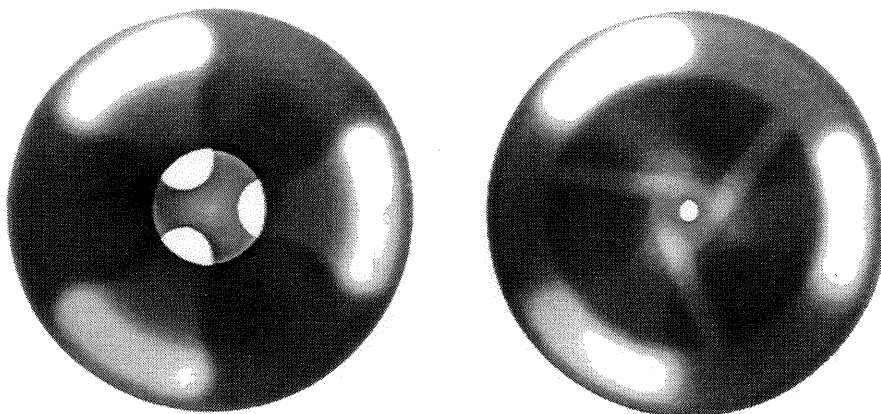


Figure 3 Back lit image of fired translucent aluminum oxide fluidic circuit allowing the well constructed interior channels to be observed.

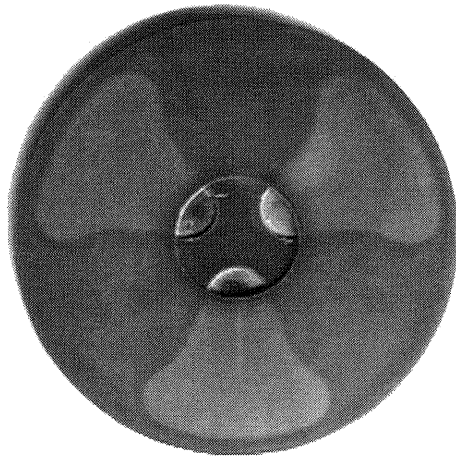


Figure 4 Fluidic circuit constructed in GS-44 silicon nitride.

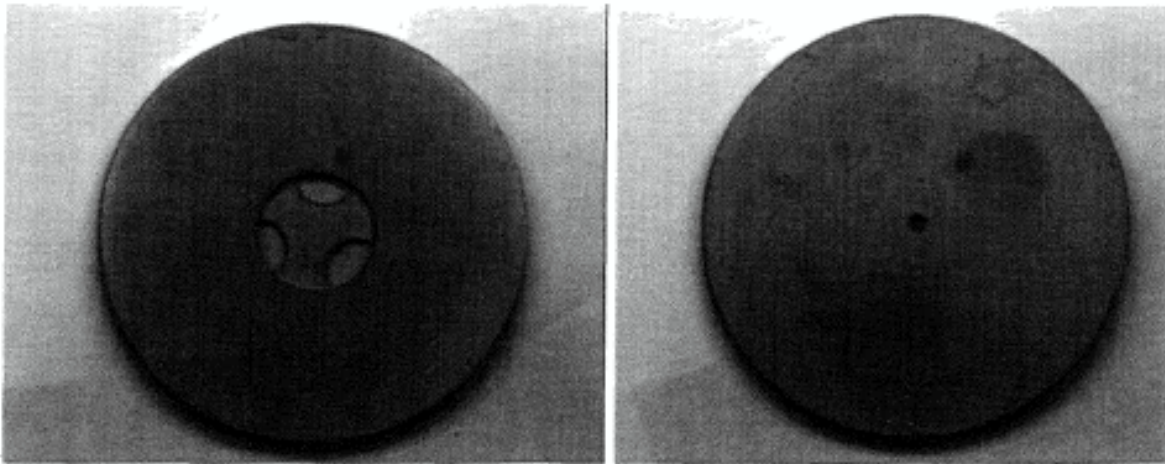


Figure 5 Fluidic circuit constructed in 316L stainless steel.

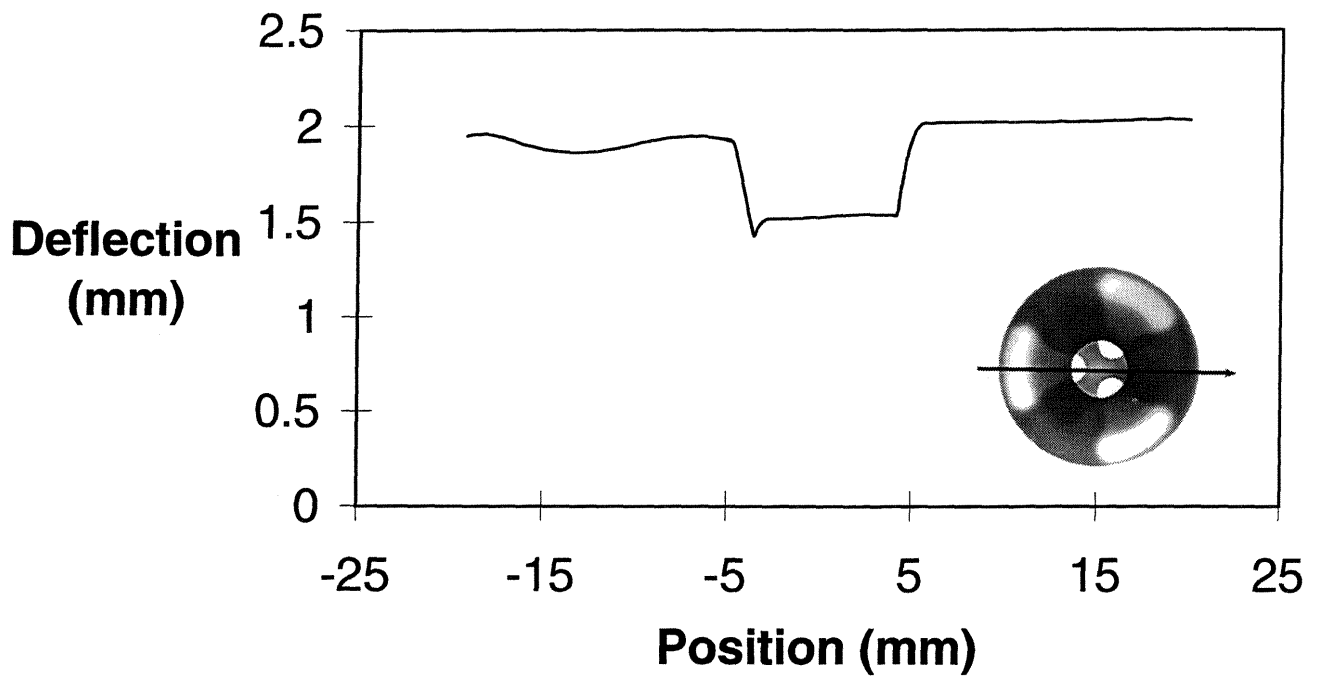


Figure 6 Images showing the direction of the coordinate measuring machine (CMM) line scan (inset) and typical results. The magnitude of the relief is unaffected by the presence or absence of the fugitive.

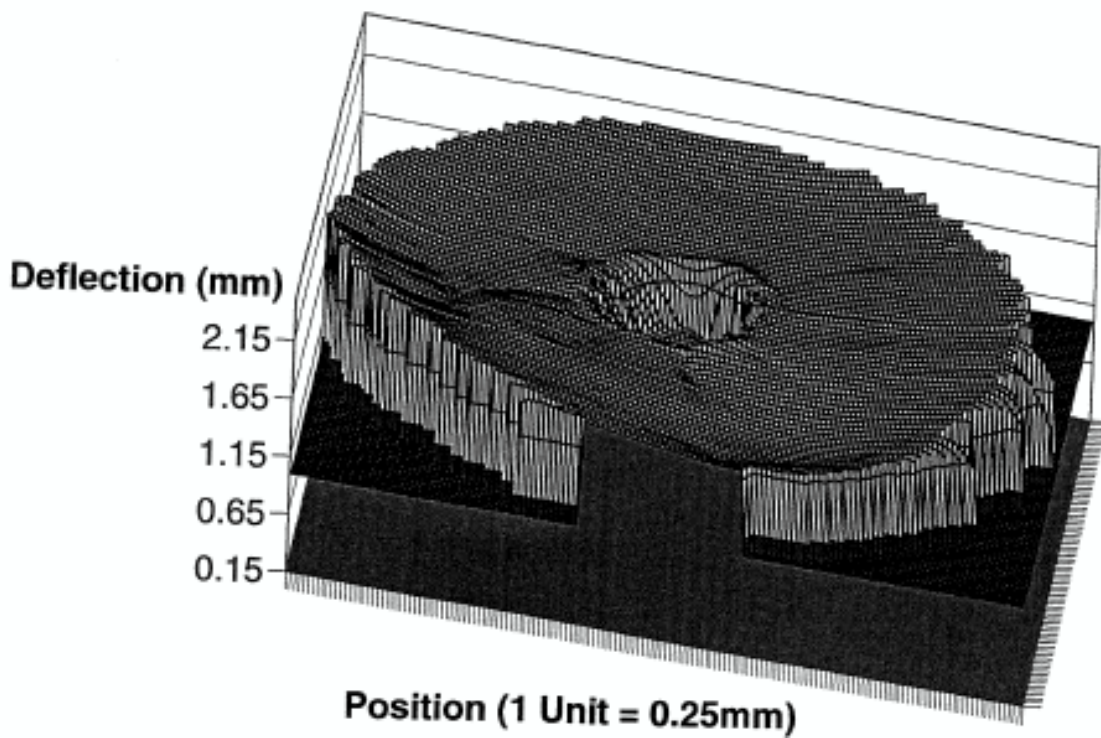


Figure 7 Relief map for the silicon nitride fluidic circuit generated using a series of parallel line scans on the CMM.

